Lab on a Chip

PAPER

View Article Online
View Journal | View Issue

Cite this: *Lab Chip*, 2022, **22**, 3521

Quantitative brain-derived neurotrophic factor lateral flow assay for point-of-care detection of glaucoma†

Yue Wu,[ab] Yubing Hu, *[a] Nan Jiang,[c] Rajeevan Anantharanjit,[bd] Ali K. Yetisen [a] and M. Francesca Cordeiro *[bdef]

Glaucoma, a ruinous group of eye diseases with progressive degeneration of the optic nerve and vision loss, is the leading cause of irreversible blindness. Accurate and timely diagnosis of glaucoma is critical to promote secondary prevention and early disease-modifying therapies. Reliable, cheap, and rapid tests for measuring disease activities are highly required. Brain-derived neurotrophic factor (BDNF) plays an important role in maintaining the function and survival of the central nervous system. Decreased BDNF levels in tear fluid can be seen in glaucoma patients, which indicates that BDNF can be regarded as a novel biomarker for glaucoma. Conventional ELISA is the standard method to measure the BDNF level, but the multi-step operation and strict storage conditions limit its usage in point-of-care settings. Herein, a one-step and a portable glaucoma detection method was developed based on the lateral flow assay (LFA) to quantify the BDNF concentration in artificial tear fluids. The results of the LFA were analyzed by using a portable and low-cost system consisting of a smartphone camera and a dark readout box fabricated by 3D printing. The concentration of BDNF was quantified by analyzing the colorimetric intensity of the test line and the control line. This assay yields reliable quantitative results from 25 to 300 pg mL^{-1} with an experimental detection limit of 14.12 pg mL^{-1}. The LFA shows a high selectivity for BDNF and high stability in different pH environments. It can be readily adapted for sensitive and quantitative testing of BDNF in a point-of-care setting. The BDNF LFA strip shows it has great potential to be used in early glaucoma detection.

Received 10th May 2022,
Accepted 2nd August 2022

DOI: 10.1039/d2lc00431c

rsc.li/loc

Introduction

Glaucoma is one of the most stimulating challenges in the field of ophthalmology, and a significant public health concern worldwide. It is estimated that approximately 111.8 million people will suffer from glaucoma by 2040.[1] Glaucoma is normally asymptomatic at the early stage and progresses slowly, and delayed diagnosis will cause irreversible vision loss.[2,3] Undoubtedly, early diagnosis of glaucoma based on effective screening programs should be a priority to prevent the progression of the disease, safeguard a patient's well-being, and reduce personal and national expenditure. Measurement of intraocular pressure (IOP) and assessing the structure of the optic nerves are routinely used in glaucoma screening.[4] Despite their effective analytical results, there is still plenty of room to improve the performance, convenience, and cost. A reliable, inexpensive, and rapid screening test is highly desired to facilitate the screening efficiency.[5] Biomarker analysis may have great potential to improve the early assessment of disease activity in glaucoma.[6] Moreover, due to noninvasive accessibility,[7] tear fluid provides an ideal platform for the biomarker detection of ocular diseases, including glaucoma. Many proteomics studies have investigated tear fluid to explore potential biomarkers for glaucoma and have demonstrated some candidates such as lysozyme C (LYZ), protein S100, immunoglobulins, prolactin-inducible protein, and phosphorylated cystatin-S (CST4).[8,9] However, none of these biomarkers show strong correlations with glaucoma onset and/or progression, and their involvement in glaucoma disease activity still needs to be

[a] *Department of Chemical Engineering, Imperial College London, South Kensington, London, UK. E-mail: yubing.hu@imperial.ac.uk*
[b] *Department of Surgery and Cancer, Imperial College London, South Kensington, London, UK. E-mail: m.cordeiro@imperial.ac.uk*
[c] *West China School of Basic Medical Sciences & Forensic Medicine, Sichuan University, Chengdu 610041, China*
[d] *The Imperial College Ophthalmic Research Group (ICORG), Imperial College London, London, UK*
[e] *The Western Eye Hospital, Imperial College Healthcare NHS Trust (ICHNT), London, UK*
[f] *Glaucoma and Retinal Neurodegeneration Group, Department of Visual Neuroscience, UCL Institute of Ophthalmology, London, UK*
† Electronic supplementary information (ESI) available. See DOI: https://doi.org/10.1039/d2lc00431c

established. Brain-derived neurotrophic factor (BDNF) plays an important role in regulating the survival, development, function, and plasticity of the nervous system.[10] Damage of the optic nerve in glaucoma leads to the interruption of retrograde transportation of BDNF which has a significant influence on further axonal dystrophy in glaucoma progression[11] (Fig. 1a). Studies have already shown that concentrations of BDNF in tears significantly decrease in both normal tension glaucoma (NTG)[12] and primary open-angle glaucoma (POAG).[13] For instance, BDNF was 116.2 ± 43.1 pg mL^{-1} in control subjects and 78.0 ± 25.1 pg mL^{-1} in POAG patients.[13] Therefore, BDNF has great potential to be regarded as an ideal biomarker for glaucoma and it is therefore necessary to develop a method to detect the BDNF tear level especially in a POC environment.

Currently, the enzyme-linked immunosorbent assay (ELISA) is the standard method to quantify the BDNF level.[14] Although it can provide accurate and convincing results, the demand for expensive instruments and well-trained technicians limits its application in point-of-care (POC) settings.[15] It is therefore highly desirable to develop a low-cost, simple and highly sensitive method for BDNF detection to help with glaucoma screening. The lateral flow assay (LFA) is a widely used paper based POC diagnostic tool and has attracted extensive interest in rapid testing due to its fast, inexpensive, and user-friendly features.[16,17] Gold nanoparticles (AuNPs) have been used for their high stability, easy conjugation with biomolecules, and strong colorimetric intensity.[18] A AuNP-based LFA has already been applied in analysis of biomarkers such as SARS-CoV-2,[19] human chorionic gonadotropin (hCG)[20] and cancer biomarkers.[21] Despite this, only a few LFA products for tear fluid analysis are available on the market. For instance, InflammaDry is a commercial device for dry eye disease that is designed to detect the concentration of matrix metalloproteinase-9 (MMP-9) in tear fluid with a limit of detection (LOD) of 40 ng mL^{-1}.[22,23] However, one of the main challenges in detecting BDNF levels in tears is the relatively low concentration which only ranges from 25.0 to 203.0 pg mL^{-1} in both glaucoma patients and healthy volunteers.[13] In addition, most of these LFA tests including InflammaDry are qualitative and merely indicate the presence/absence of the analyte.[24] Finally, the levels of BDNF differ in different stages of POAG: 56.8 ± 10.3, 92.4 ± 34.9, 80.1 ± 20.4, and 76.7 ± 20.2 pg mL^{-1} in the early, moderate, advanced and severe stages respectively.[13] Quantitative detection of tear BDNF can differentiate the severity and the stage of glaucoma. Therefore, optimizing the component materials, improving the properties of the label and designing a sensitive read system are necessary to fabricate a highly sensitive quantitative LFA for the detection of BDNF.

In this study, a LFA strip was developed as a portable analytical device for the rapid and quantitative detection of BDNF in tear fluid for the first time. The design of the LFA

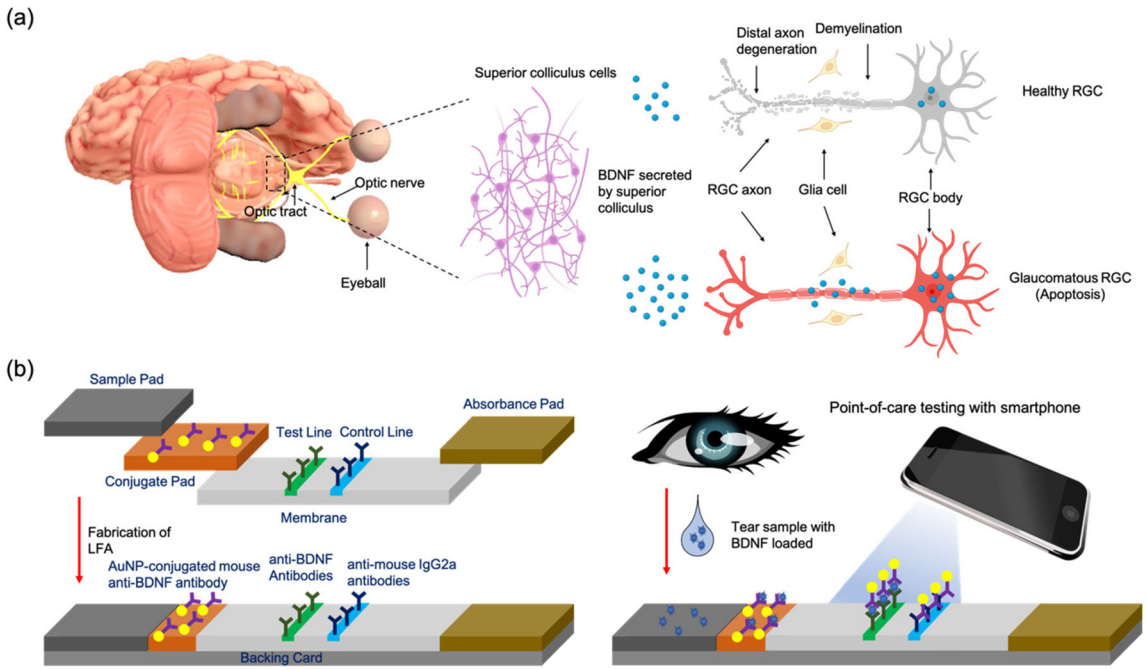

Fig. 1 Schematic illustrating the devices used to test the concentration of BDNF in tears. a) The illustration indicates the glaucomatous changes of the transports of BDNF. BDNF is generated in the superior colliculus and retrogradely transported to the retinal ganglion cell body through axons. Glaucomatous damage leads to apoptosis of RGCs and the disruption of the BDNF transport to retinal ganglion cells. b) The illustration indicates the mechanism of the LFA device. A liquid sample with BDNF is loaded into the sample pad and migrates to a conjugate pad. The conjugate pad is impregnated with AuNP labeled antibodies which can interact with analytes in the sample. The labelled analytes then migrate to the reaction membrane where antibodies for the desired analyte are fixed at a certain area (test line). Images of the LFA strip are captured using a smartphone camera. The concentration of BDNF is quantified by measuring the colorimetric intensity.

strip for BDNF detection is shown in Fig. 1b. Specifically, capture anti-human BDNF antibodies and rabbit anti-mouse IgG2a antibodies were dispensed into a reacting membrane to serve as the test line and the control line, respectively (Fig. 1b). Detective anti-human BDNF antibodies were conjugated with AuNPs and loaded on a conjugate pad. A 40 nm AuNP was chosen to serve as the colorimetric reporter size because of its higher sensitivity compared with other AuNP sizes.[25,26] The optimal concentration of detective antibodies and pH values were studied. After adding the artificial tear fluid containing BDNF to the LFA strip, red bands were observed at the test line and the control line. The red band in the test zone indicated the existence of BDNF and its concentration was analyzed by calculating the delta RGB, which was believed to provide a consistent correlation with antigen concentration in a single color shift test.[27] An optical analyzing system consisting of a smartphone camera and a readout box was used to measure the intensity to quantify the concentration of BDNF. The presence of a red band on the control line demonstrated the feasibility of the LFA strip. The selectivity, stability, and recovery were verified to detect BDNF levels in tears and reflect the disease activity of glaucoma at POC settings.

Results and discussion

BDNF detection by commercial ELISA

ELISA is regarded as a standard method to quantify target antigens or antibodies in a biological sample based on the antigen–antibody interaction.[28,29] The target analyte was fixed by the capture antibodies. The detective antibodies were combined with horseradish peroxidase (HRP) which can interact with 3,3′,5,5′-tetramethylbenzidine (TMB) to produce color changes (Fig. S1a†). A microplate reader was used to measure the colorimetric intensity through absorption.[29] To obtain a standard curve, standard samples with BDNF concentrations of 1000, 500, 250, 125, 62.5, 31.25, and 15.63 pg mL^{-1} were prepared over serial dilutions. Absorbance spectra were collected at a wavelength range from 400–550 nm. The results showed that the absorbance peak was located at 450 nm and there was a positive relationship between the absorbance maximum and the BDNF

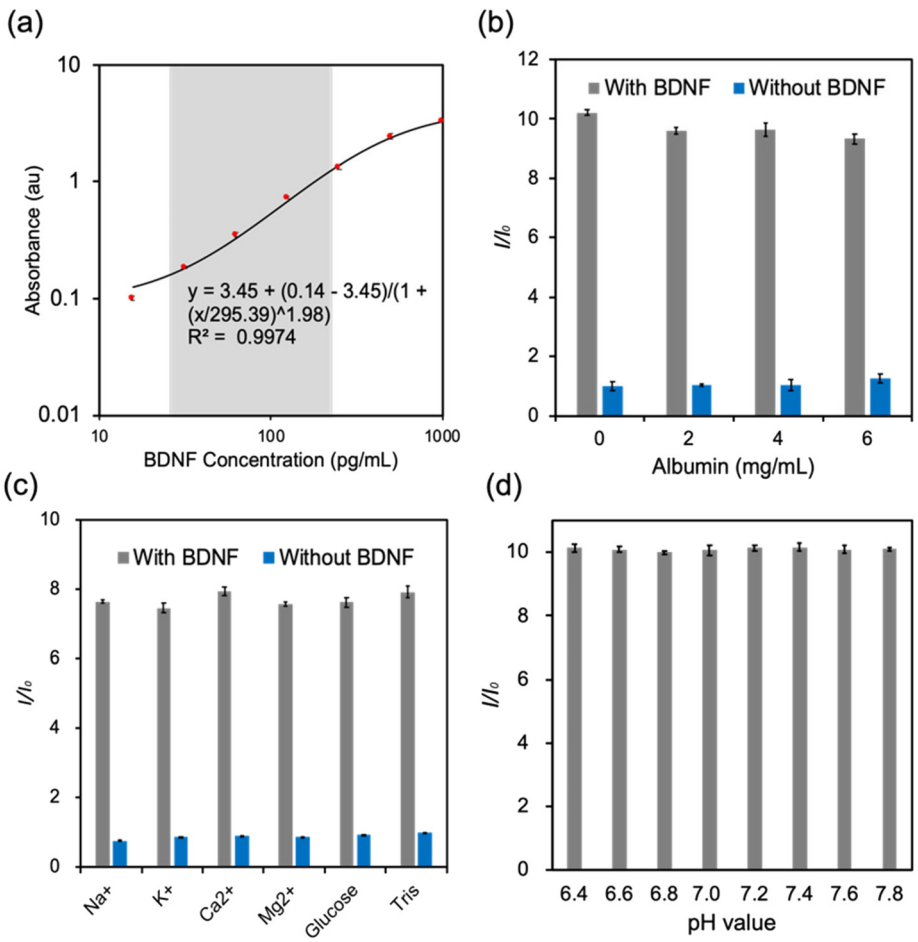

Fig. 2 Measurement of the human BDNF ELISA kit. a) Human BDNF standard curve for the ELISA test. b) The selectivity test for albumin. BDNF samples (concentration of 200 pg mL^{-1}) and Tris buffer were prepared and contained albumin at different concentrations (0, 2, 4, 6 mg mL^{-1}). c) The absorbance signal of the sample with common ions including Na^+, K^+, Ca^{2+}, Mg^{2+}, and glucose. d) The effect of pH value (6.4–7.8) of artificial tear fluid on the ELISA test with a BDNF concentration of 200 pg mL^{-1}. Error bars represent the standard error of the mean (SEM). n = 3.

concentration (Fig. S1b†). The absorption peak readings at a wavelength of 450 nm were plotted into a four-parameter logistic (4PL) curve model and R^2 = 0.9974 indicated that the curve fitted the data points well (Fig. 2a).

To detect the selectivity of the human BDNF ELISA kit, different constituents were selected, and they were albumin, Na^+, K^+, Ca^{2+}, Mg^{2+}, and glucose. A control detection was firstly performed to detect the effect of albumin at 3 different concentrations (Fig. 2b). The results indicated that albumin displayed no obvious influence on the absorption of both BDNF and blank solutions. The selectivity tests of the BDNA ELISA kit in response to electrolytes and glucose demonstrated that these analytes had negligible interference in the BDNF detection (Fig. 2c). A pH-dependence study was conducted at a pH range of 6.4–7.8 with 200 pg mL^{-1} BDNF. The results showed that the absorbance was similar at different pH values, illustrating that pH variation in the sample solutions would not affect the accuracy of ELISA (Fig. 2d). Therefore, this ELISA test was not only highly accurate but also very selective. Moreover, the results were not affected by the pH value of the sample which may indicate that it could be used in a wide range of samples. However, the requirement of sophisticated equipment such as a microplate reader or a spectrophotometer, as well as frozen storage, significantly limited its usage in POC settings.

Fabrication and conjugation of LFA

The conjugate pad is one of the key parts of an LFA strip. The target analytes that flow from the sample pad can combine with the detective antibodies labelled by colorimetric components. AuNPs are one of the widely used labels in the fabrication of LFA strips due to their stability, high binding affinity to biomolecules, and clear optical signal.[30] Studies showed that AuNPs with a size of around 40 nm exhibited superior performance for the LFA.[25,31] It is acknowledged that antibodies can be adsorbed onto AuNPs and physisorption is the simplest approach[32] (Fig. S2a†). The

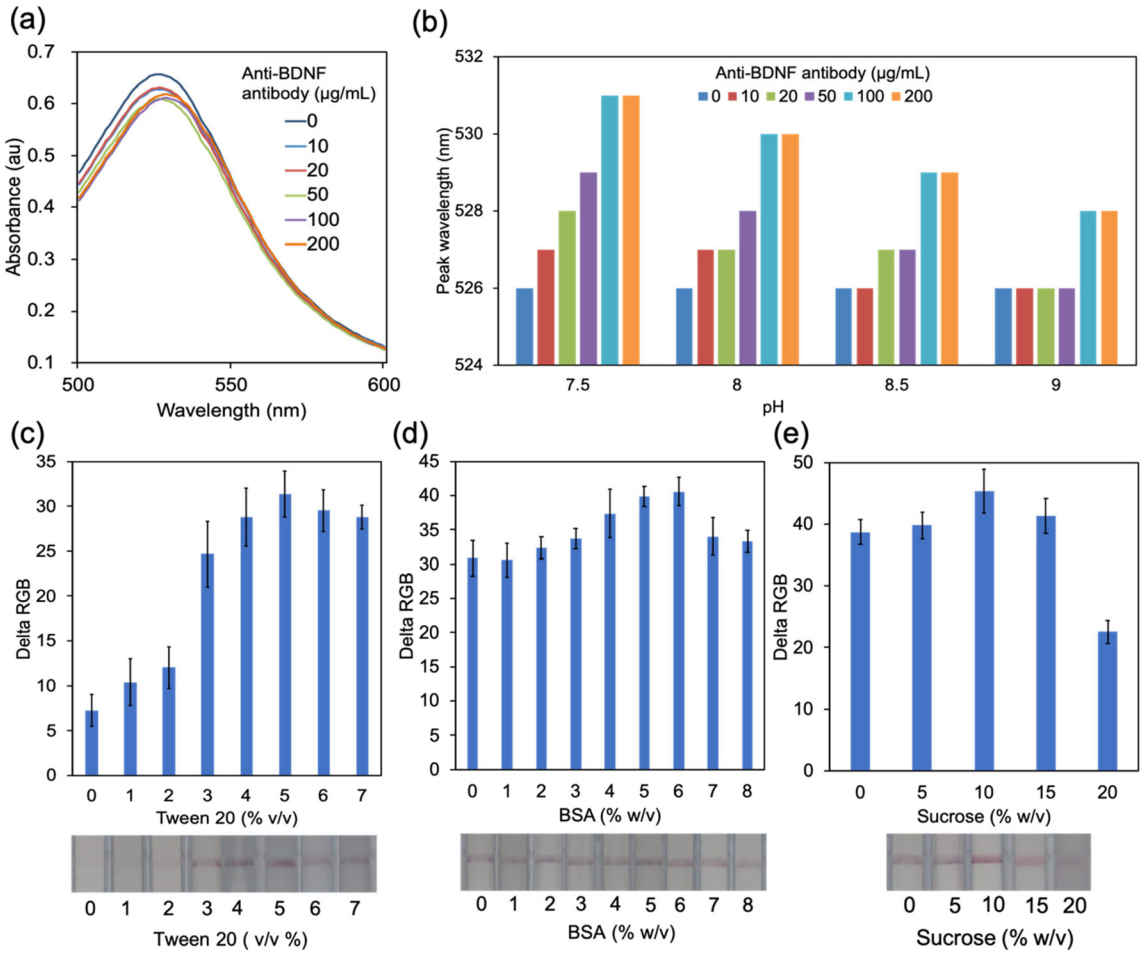

Fig. 3 Optimization of AuNP–antibody conjugation and conjugate pad treatment. a) The absorbance spectra of the resulting antibody–AuNP conjugate solutions at pH 7.5. b) The peak wavelengths of different solutions. c) The resulting delta RGB values of the control line by treating the conjugate pad with different concentrations of Tween 20. d) The resulting delta RGB values of the control line by treating the conjugate pad with different concentrations of BSA. e) The resulting delta RGB values of the control line by treating the conjugate pad with different concentrations of sucrose.

isoelectric point (pI) and volume of the antibodies as well as the pH value of the AuNP solution play important roles in physisorption.[32] It is critical to find the optimal pH value which is close to or slightly above the pI to provide a suitable environment for AuNP–antibody conjugation. Different volumes of detective anti-antibodies were added into AuNP solutions with different pH values. The absorbance peak was then determined using a microplate reader. The absorbance peak of pure AuNPs appeared at 526 nm when changing the pH from 7.5 to 9, while the peak redshifted at different levels after adding 10 μL of BDNF antibody solutions with concentrations ranging from 10 to 200 μg mL^{-1} (Fig. 3a and b and S2b–d†). It is believed that the redshift is caused by the conjugation between AuNPs and antibodies and the resultant increase of the diameter of the conjugate.[33] The largest peak shift occurred when 100 or 200 μg mL^{-1} BDNF antibody solution was added to 190 μL AuNP solution at pH 7.5 (Fig. 3a and b), which indicated that the optimal pH of conjugation was 7.5.

Pre-treatment of the conjugate pad is necessary because appropriate buffer treatment could ensure a smooth and rapid release of the analyte from the conjugate pad.[34] Normally, there are 3 major components in the treatment buffer: bovine serum albumin (BSA), sucrose, and Tween 20 (Fig. S2a†). BSA is used to reduce the unspecific binding between AuNP–antibody conjugates and the conjugate pad. Tween 20 is a common detergent that is used to minimize the unspecific binding as well as to facilitate the flow of the analyte.[35] Sugar (such as sucrose) is the key component in the conjugate pad treat buffer to preserve the biological activity and function of the detective antibodies by forming a layer at the surface of AuNP–antibody conjugates to keep the structure and the binding site.[35,36] Moreover, sucrose is believed to have a positive effect on the flow of the analyte because the sucrose layer dissolves immediately and works as a carrier of the detector to enter the fluid stream.[36,37] The effect of Tween 20 was firstly detected by testing the performance of the solution with Tween 20 concentrations from 1 to 7% (v/v). BSA with a concentration of 1–8% (w/v) was then added to the solution with optimal Tween 20 concentration. Finally, sucrose was added to the mixture. The delta RGB values of control lines were calculated to reflect the release of the conjugate pad after treating with the buffer. The results showed that the buffer which contained 5% v/v Tween 20, 6% w/v BSA and 10% w/v sucrose could help to improve the release of the conjugate, which, subsequently, presents a line with higher intensity in the membrane (Fig. 3c–e).

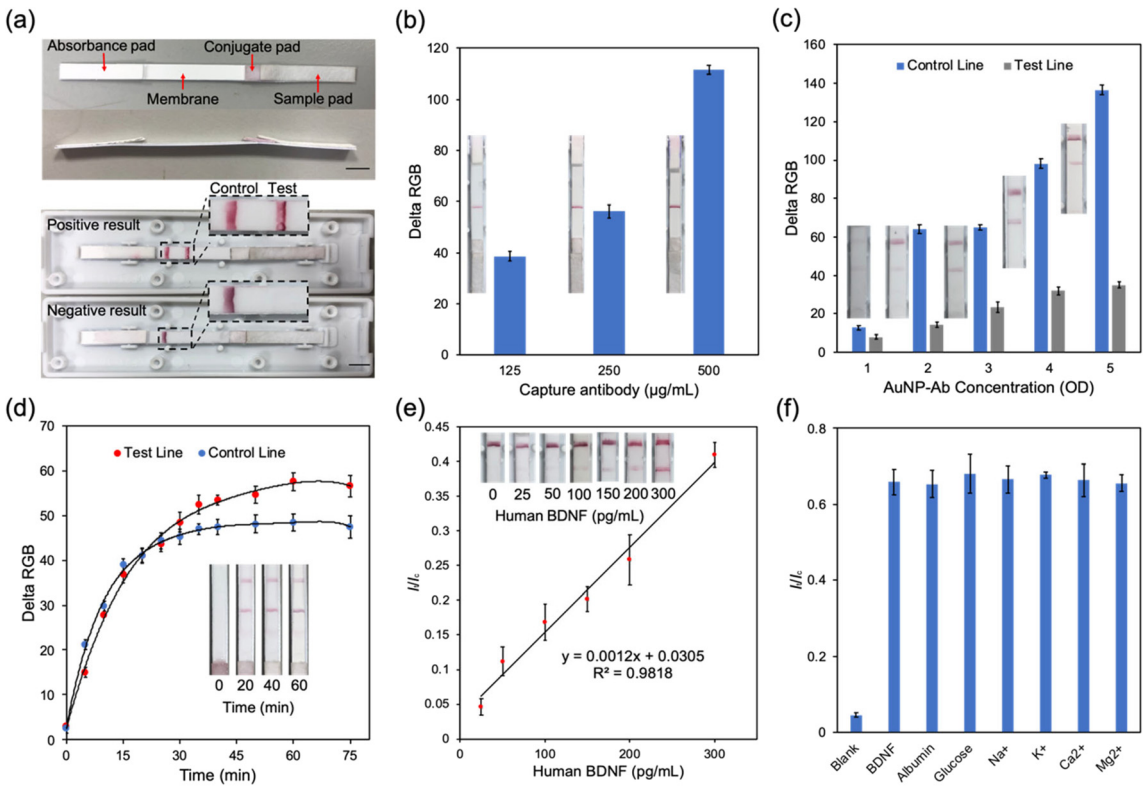

Fig. 4 BDNF lateral assay strip test in Tris buffer. a) Image of the BDNF LFA test strip and possible test results. The strip consists of a sample pad, a conjugate pad, a reaction membrane and an absorbance pad. All pads are assembled in a backing. The scale bar represents 5 mm. b) The delta RGB values of the test line in different test strips with capture antibodies at different concentrations (125, 250 and 500 μg mL^{-1}). c) The delta RGB values in different test strips when loading different volumes of AuNP–antibody conjugates. d) The delta RGB values after a certain time. e) The linear relationship between BDNF concentration and I_t/I_c. I_t/I_c = delta RGB_{tl}/delta RGB_{cl}. f) The effect of certain compositions on the BDNF LFA strip. Error bars represent the standard error of the mean (SEM). $N \geqq 3$.

Optimization of the BDNF LFA strip in Tris buffer

To fabricate the LFA strip, a pretreated sample pad, conjugate pad and absorbance pad were assembled in a backing card with a 2 mm overlap (Fig. 4a).[37] A red test line and a red control line were the positive results and only one line at the control area represented the negative result (Fig. 4a). The volume of capture antibodies dispensed in the test zone affected the colorimetric intensity of the result. Fig. 4b shows that loading of 500 μg mL^{-1} capture antibody solution could catch more BDNF. The amount of AuNP–antibody conjugates was also varied by tuning the volume to evaluate its effect on the colorimetric intensity difference of the control line and the test line (Fig. 4c). The concentration of the AuNP–antibody conjugates could be controlled through resuspending the conjugate with a different volume of PBS

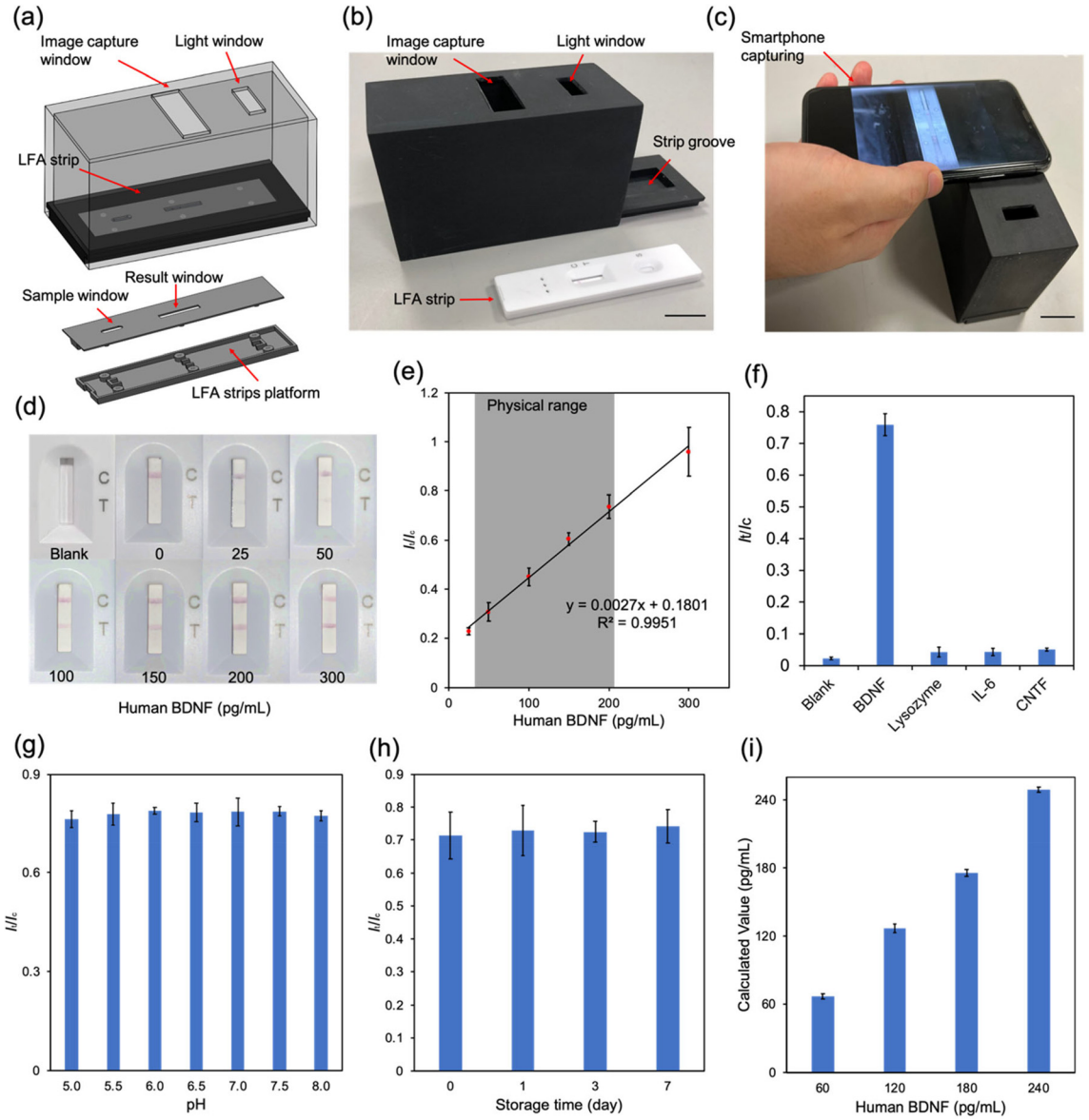

Fig. 5 BDNF detection in artificial tear fluid with the BDNF LFA strip. a) Schematic illustration of the readout system. b) Real image of the readout system. The scale bar represents 4 cm. c) Image of capturing LFA images through a smartphone camera. The scale bar represents 2 cm. d) Image of the reading area of the strips before and after loading artificial tear fluid samples with different volumes of BDNF. e) The linear relationship between I_t/I_c and concentration of BDNF. f) I_t/I_c values after loading artificial tear fluid containing different proteins including lysozyme, IL-6, CNTF and BDNF. The concentration of lysozyme was 2.36 mg mL^{-1}, the concentration of IL-6 was 30 pg mL^{-1}, the concentration of CNTF was 60 pg mL^{-1} and the concentration of BDNF was 200 pg mL^{-1}. g) I_t/I_c values after loading artificial tear fluid samples with a BDNF concentration of 200 pg mL^{-1} at different pH values. h) I_t/I_c values after loading artificial tear fluid samples with a BDNF concentration of 200 pg mL^{-1} onto strips stored in the lab environment for 0, 1, 3, and 7 days. i) The recovery test of artificial tear fluid with a concentration 60, 120, 180 and 240 pg mL^{-1}. The calculated values are 66.74, 126.68, 175.31 and 249.29 pg mL^{-1} and the recoveries of each group are 88.76%, 105.57%, 97.39% and 103.87%, respectively. Error bars represent the standard error of the mean (SEM). $N \geqq 3$.

solution. In this test, the AuNP–antibody conjugates were resuspended to 1 to 5 OD. The colorimetric intensity of both the test line and control line increased with the increased concentration of conjugates. A lower duration allows a test to be more acceptable in screening settings. However, it required time to allow adequate reaction between BDNF and capture anti-BDNF antibodies in the test zone. In our study, the colorimetric intensity reached the stable stage in 30–45 minutes (Fig. 4d) which indicated that the results should be captured at least after 30 minutes.

To figure out the relationship between I_t/I_c, which represents the ratio of delta RGB values of the test line and control line, and the BDNF concentration, different volumes of BDNF were dissolved in Tris buffer to produce a series of buffer solutions from 0 to 300 pg mL^{-1} (Fig. 4e). All samples were loaded at the sample pad and the results were analyzed. It could be easily identified by the naked eye that the colorimetric intensity of the test line got stronger as the BDNF concentration increased. I_t/I_c was plotted on the Y axis and the BDNF concentration on the X axis to generate a standard curve with R^2 = 0.98 (Fig. 4e). To better mimic the real situation for human tear fluid tests, the performance of the LFA strip was tested in artificial tear fluid, which was made from Tris buffer and contained NaCl, KCl, $CaCl_2$, $MgCl_2$, albumin, and glucose.[38] A selectivity experiment was therefore necessary to test the effect of these components on the LFA strip by performing the LFA test with different BDNF samples, containing each component (Fig. 4f). The results showed no obvious influence from these components.

BDNF LFA strip performance in artificial tear fluid

Smartphone cameras provide an ideal alternative option to a traditional flatbed scanner or a CCD camera required in quantifying LFA results.[39] To reduce the environmental interference, a dark readout box was designed (Fig. 5a and b). The readout box was produced by 3D printing and consisted of an image capture window, an extra light window and a lid with a groove at the center to hold the LFA. The whole system was highly portable and cost-effective which made it suitable in POC settings. As shown in Fig. 5c, the colorimetric intensity of the test line was enhanced with the increase of BDNF concentration in artificial tear fluid. The I_t/I_c values confirmed the linear connection of BDNF concentrations ranging from 0 to 300 pg mL^{-1} in artificial tear fluid with a detection limit of 14.12 pg mL^{-1} (Fig. 5d and e). The range of BDNF levels in glaucoma patients and normal subjects is around 40 to 200 pg mL^{-1},[13] which indicated that the BDNF LFA strip was suitable to be used in detecting BDNF levels in human tears.

Although not all pathogenic mechanisms of glaucoma are well understood, certain factors involved in the disease process have been identified. These include neurodegeneration, immune reaction, ischemia, and oxidative stress.[40] Selectivity tests were performed on several molecules previously identified as being involved in glaucomatous processes including lysozyme,[41] IL-6 (ref. 42) and CNTF.[43] As shown in Fig. 5f, only samples with BDNF produced a positive result with a high I_t/I_c value, while other molecules only resulted in negative readings. These results demonstrated that our LFA strip had a high specificity to BDNF. The pH value of tear fluid is one of the important factors that may affect the accuracy of the LFA test. It has been reported that the pH of tears from normal subjects ranges from 6.5 to 7.6,[44] and can be more acidic with certain disorders or medication usage such as in glaucoma.[45,46] Therefore, artificial tear fluid samples containing 200 pg mL^{-1} BDNF with different pH values from 5.0 to 8.0 were prepared and tested with LFA strips. The results demonstrated the negligible effect of pH on the final readings. This means that the test strip can be reliably employed for BDNF detection from tears in patients with various medical conditions and on medications that can affect the pH of the tear film (Fig. 5g).

Long lifespan and stability are some key advantages of the LFA strip. The effect of storage time on the performance of the LFA strip was further investigated by loading an artificial tear sample with 200 pg mL^{-1} BDNF onto strips which were stored at room temperature for 1, 3, and 7 days and the I_t/I_c values were calculated. As shown in Fig. 5h, the results were the same for different storage times. In order to determine the accuracy of the BDNF LFA strips, artificial tear fluid samples with BDNF concentrations of 60, 120, 180 and 240 pg mL^{-1} were prepared and tested as controls. The final results were 66.74, 126.68, 175.31 and 249.29 pg mL^{-1}, respectively, with increasing BDNF concentrations (Fig. 5i). The results indicated the ability of the BDNF LFA strip to sensitively measure the BDNF level in artificial tear fluid with high accuracy. In summary, the LFA strip is an ideal diagnostic tool for glaucoma as the test is portable, practical, quick, convenient and cost-effective.

As far as we are aware, the human BDNF LFA strip is the first to quantify the BDNF level in liquid samples in a POC setting. Due to the noninvasive collection method, tear fluid is regarded as an ideal source for the biomarkers of the disease.[47,48] There has been increased interest in investigating novel tear biomarkers for ocular diseases.[49] BDNF plays an important role in the homeostasis of the central nervous system.[50] Compared to that of other biomarkers, the role of BDNF in glaucoma has been clearly demonstrated by many different studies, as summarized in Table S1.† There is strong evidence proving that changes in BDNF are involved in the early pathogenic stages of glaucoma including retinal ganglion cell apoptosis and axonal dystrophy.[51] A decrease of retrograde transportation of BDNF from the brain to the retina has been established in several animal models of glaucoma,[52–54] whilst exogenous BDNF has been shown to be neuroprotective to injured RGCs.[55] Several clinical studies have identified significantly reduced serum levels of BDNF in glaucoma patients compared with those in healthy volunteers.[56–58] Recently, Shpak *et al.* presented quantitative results of BDNF levels in tear fluid showing a level of 78.0 ± 25.1 pg mL^{-1} in patients with POAG,

compared to those in control subjects (116.2 ± 43.1 pg mL^{-1}).[13] Moreover, the study demonstrated that the tear level of BDNF was the lowest in the patients in the earliest stages of the disease (56.8 ± 10.3 pg mL^{-1}).[13] Our BDNF LFA strip showed great selectivity and stability with a reasonable detection range from 14.12 to 300 pg mL^{-1} which is comparable to that of a commercial ELISA kit and covers both physiological and glaucomatous ranges of BDNF level in tears. Furthermore, it allows the LFA strip to detect abnormally low BDNF levels in tear fluid reported in the early stages of glaucoma.

Conventional ELISA shows a great ability to detect BDNF in tear fluid with a wide range of detection, high reproducibility, recovery and selectivity (Table S2†), but the complex operating steps limit its use in POC settings. Other biomarker detection methods such as gel electrophoresis-based immunoassay, fluorometric immunoassay, and radioimmunoassay also have similar problems.[15] However, our human BDNF LFA strip showed a comparable performance to that of a conventional ELISA kit. The intra-assay CV was 7.6% and the inter-assay CV was 9.0% which demonstrated the great repeatability of the LFA (Table S2†). Notably, the operating protocol of the LFA strip is much simpler, being a one-step procedure. Without the washing and incubation steps, the response time of our BDNF LFA strip is only 30 to 40 minutes whereas an ELISA kit requires 90 minutes to several hours (Table S2†).

InflammaDry is a commercially available LFA device designed to detect matrix metallopeptidase 9 (MMP-9)[9] in tear fluid. Sambursky *et al.* demonstrated that the sensitivity and specificity of InflammaDry were 85% and 94%, respectively. The negative predictive value was 73% and positive predictive value was 97%.[22] Another group developed a LFA device to detect trachoma based on the antibody against *Chlamydia trachomatis*.[59] However, both InflammaDry and the LFA for trachoma detection are qualitative. We introduced a quantitative system consisting of a dark box, a smartphone camera and the computer software ImageJ to quantify the concentration of BDNF in fluid samples. Our LFA strip shows great accuracy by testing samples with a known BDNF concentration, as well as having high reproducibility and selectivity. Importantly, the strip can be stored in normal environments which significantly decreases the storage cost and improves the practicality of the testing kit.

Our results show that the BDNF LFA strip has potential to quantitatively measure BDNF levels in tear fluid in POC settings without the need for other sophisticated equipment. However, it is important to recognize that this prototype needs more research and testing. To reduce the error caused by manual analysis of the results, a smartphone app will be developed to simplify obtaining the results. More glaucoma biomarkers such as ciliary neurotrophic factor (CNTF)[43] and homocysteine (Hcy)[60] can be added to the strip to achieve the goal of multiplexed quantification and improve the sensitivity of the test for detection of glaucoma.

Conclusion

In summary, a AuNP based human BDNF LFA strip can measure BDNF levels up to 300 pg mL^{-1} in artificial tear fluid. The LFA strip provides a short response time of 30 to 40 minutes with a detection limit of 14.12 pg mL^{-1}, which makes this testing kit ideal for POC settings. The smartphone based readout system and the software ImageJ were able to quantify the BDNF concentration based on the colorimetric signal. The strip shows great selectivity and stability. Moreover, the test strips are proved to stay stable for testing artificial tear samples with different pH values, which indicates that the assay is able to obtain reliable results from tears of every patient including those who are under certain medications. All these properties demonstrate that the BDNF LFA strip is highly capable and could be manufactured in large scale to detect the BDNF levels in real human tears. With the development of an automatic reading app based on smartphones, the test could be more accessible and easier to use, even in non-clinical settings, *i.e.*, at homes. Combining the LFA strip with tear collection devices is one of the future plans to decrease the error caused during the sample collection. The strip needs to be tested in a real environment to estimate its performance in glaucoma screening. All in all, the BDNF LFA test establishes great potential to be used in screening of glaucoma.

Materials and methods

Materials and instruments

A human BDNF ELISA kit, recombinant anti-mouse IgG2a antibodies, and recombinant human BDNF protein were obtained from Abcam. Albumin, bovine serum albumin, calcium chloride, glucose, gold nanoparticles (40 nm), magnesium chloride, potassium chloride, sucrose, Tween 20, sodium chloride, Tris-hydrochloride and Tris base were obtained from Sigma-Aldrich. Two different anti-Human BDNF antibodies were purchased from R&D Systems. All components of the lateral flow test strip, including the backing, sample pad, conjugate pad, reacting membrane and absorbent pad were obtained from Whatman. The absorbance spectrum was measured through a microplate reader (Varioskan LUX Multimode, ThermoFisher). The test line and control line were dispensed using a syringe pump (KDS-200-CE, KD Scientific Inc.). The readout box was produced using a 3D printer in Chemical Engineering Workshop. The images were captured using an iPhone X.

Fabrication and assay procedure of the paper-based ELISA

The nitrocellulose membrane was firstly cut into discs 5 mm in diameter. 5 μL capture antibody solution was pipetted on each disc and the discs were incubated for 1 hour at 37 °C. Each disc was washed with washing buffer 3 times to remove unbound antibodies. 5 μL of 5% BSA buffer was pipetted to each disc and incubated at 37 °C for 1 hour to block the

paper plate and reduce unspecific binding. Each disc was washed again 3 times. The fabrication of paper-based plates was now complete and they were ready for ELISA. Firstly, 5 μL of the sample solutions containing different concentrations of BDNF were pipetted to each disc. After 10 min incubation, the discs were washed 3 times. Then, 5 μL of horseradish peroxidase (HRP)-labeled detective antibodies was added to each disc and allowed to incubate for 10 minutes. The discs were washed 3 times again. 5 μL of 3,3′,5,5′-tetramethylbenzidine (TMB) substrate solution was added to each disc and finally, 5 μL of stop solution was pipetted to each disc.

Gold nanoparticle (AuNP) and anti-BDNF antibody conjugation

The pH of AuNP solution was firstly adjusted to 7.5, 8.0, 8.5 and 9.0. 190 μL of AuNP solution with different pH values was added into 1.5 mL microtubes. 10 μL of anti-BDNF antibody solution (concentration range from 10, 20, 50, 100, 200 μg mL^{-1}) was added to the relevant microtubes. To allow the conjugation between AuNPs and antibodies, the mixtures were incubated for 30 minutes at room temperature. After incubation, the AuNP–antibody solution was centrifuged for 10 minutes. The supernatant was removed, and the conjugate was resuspended in 200 μL with PBS solution. The centrifugation step was repeated 3 times. To assess the conjugation between AuNPs and antibodies, the absorbance spectrum of each conjugation solution was then detected using a microplate reader.

Fabrication of BDNF LFA strips

Each part was cut using a FOBA laser. The sample pad was treated with Tris buffer containing Tween 20 and BSA. The conjugate pad was pre-treated with the conjugate pad buffer. 15 μL AuNP–antibody conjugate was loaded into the conjugate pad. The detective anti-human BDNF antibodies were dispensed into the test line at the membrane using a syringe and pump. The anti-mouse IgG2a antibodies were loaded at the control line in the membrane. All parts of the LFA strips were assembled at a backing with a 2 mm overlap finally.

Performing the LFA test and testing the performance

A BDNF sample was prepared in Tris buffer and artificial tear fluid. Before loading to the sample pad, 10 μL of sample was mixed with 60 μL running buffer. The mixture then was loaded at the sample pad. After waiting for 30 minutes, the results were captured using an iPhone X in the readout box. To test the effects of the composition of artificial tears, certain components (150 mM NaCl, 20 mM KCl, 1.0 mM $CaCl_2$, 0.6 mM $MgCl_2$, 3.94 mg mL^{-1} albumin and 0.14 mM glucose) were added into Tris buffer separately. The LFA test was performed using these samples with different compositions and the colorimetric intensities were analyzed. To test the LFA performance in artificial tears, the pH was considered as a factor which may influence the results. The adjusted pH of artificial tear fluid ranged from 5.0 to 8.0. Artificial tear samples with different pH values were tested. The recovery test was performed by loading samples with a concentration of 60, 120, 180 and 240 pg mL^{-1} BDNF. The results were calculated by using the standard curve and compared with the known value. The performance of the LFA strips after day 1, day 3 and day 7 was also tested.

Image capture and data analysis

The image capture box and LFA case were made by 3D printing. The images were captured using an iPhone X. The RGB values of selected bands were obtained with ImageJ. The delta RGB values were then calculated on an Excel spreadsheet using the below equation (eqn (1)).

$$\Delta RGB = \sqrt{(R-R_0)^2 + (G-G_0)^2 + (B-B_0)^2} \quad (1)$$

The subscript 0 corresponds to the background.

The limit of detection (LOD) was calculated using eqn (2).

$$\text{LOD} = \text{Mean of blank data} + 3 \times (\text{Standard deviation of blank data}) \quad (2)$$

The coefficient of variation (CV%) was calculated using eqn (3)

$$\text{CV\%} = \text{Standard deviation/Mean} \quad (3)$$

The results were shown as I_t/I_c to reduce the effects of environment light contamination. Each group contained at least 3 strips. The error bars represented the SEM (standard error of the mean).

Conflicts of interest

There are no conflicts to declare.

Acknowledgements

A. K. Y. and Y. H. thank the Engineering and Physical Sciences Research Council (EP/T013567/1). N. J. acknowledges the National Natural Science Foundation of China (No. 82102182) and the Fundamental Research Funds for the Central Universities (No. YJ202152).

References

1 Y. C. Tham, X. Li, T. Y. Wong, H. A. Quigley, T. Aung and C. Y. Cheng, Global prevalence of glaucoma and projections of glaucoma burden through 2040: a systematic review and meta-analysis, *Ophthalmology*, 2014, **121**, 2081–2290.

2 R. N. Weinreb, T. Aung and F. A. Medeiros, The pathophysiology and treatment of glaucoma: a review, *JAMA*, 2014, **311**, 1901–1911.

3 M. F. Cordeiro, E. M. Normando, M. J. Cardoso, S. Miodragovic, S. Jeylani, B. M. Davis, L. Guo, S. Ourselin, R.

A'Hern and P. A. Bloom, Real-time imaging of single neuronal cell apoptosis in patients with glaucoma, *Brain*, 2017, **140**, 1757–1767.

4 J. R. McManus and P. A. Netland, Screening for glaucoma: rationale and strategies, *Curr. Opin. Ophthalmol.*, 2013, **24**, 144–149.

5 E. A. Maul and H. D. Jampel, Glaucoma screening in the real world, *Ophthalmology*, 2010, **117**, 1665–1666.

6 S. McNally and C. J. O'Brien, Metabolomics/Proteomics strategies used to identify biomarkers for exfoliation glaucoma, *J. Glaucoma*, 2014, **23**, S51–S54.

7 S. Hagan, E. Martin and A. Enriquez-de-Salamanca, Tear fluid biomarkers in ocular and systemic disease: potential use for predictive, preventive and personalised medicine, *EPMA J.*, 2016, **7**, 15.

8 A. Fernández-Vega Cueto, L. Álvarez, M. García, A. Álvarez-Barrios, E. Artime, L. Fernández-Vega Cueto, M. Coca-Prados and H. González-Iglesias, Candidate Glaucoma Biomarkers: From Proteins to Metabolites, and the Pitfalls to Clinical Applications, *Biology*, 2021, **10**, 763.

9 Y. Wu, M. Szymanska, Y. Hu, M. I. Fazal, N. Jiang, A. K. Yetisen and M. F. Cordeiro, Measures of disease activity in glaucoma, *Biosens. Bioelectron.*, 2022, **196**, 113700.

10 B. A. Mysona, J. Zhao and K. E. Bollinger, Role of BDNF/TrkB pathway in the visual system: Therapeutic implications for glaucoma, *Expert Rev. Ophthalmol.*, 2017, **12**, 69–81.

11 M. Almasieh, A. M. Wilson, B. Morquette, J. L. Cueva Vargas and A. Di Polo, The molecular basis of retinal ganglion cell death in glaucoma, *Prog. Retinal Eye Res.*, 2012, **31**, 152–181.

12 A. Ghaffariyeh, N. Honarpisheh, Y. Shakiba, S. Puyan, T. Chamacham, F. Zahedi and M. Zarrineghbal, Brain-derived neurotrophic factor in patients with normal-tension glaucoma, *Optometry*, 2009, **80**, 635–638.

13 A. A. Shpak, A. B. Guekht, T. A. Druzhkova, K. I. Kozlova and N. V. Gulyaeva, Brain-Derived Neurotrophic Factor in Patients with Primary Open-Angle Glaucoma and Age-related Cataract, *Curr. Eye Res.*, 2018, **43**, 224–231.

14 M. Bockaj, B. Fung, M. Tsoulis, W. G. Foster and L. Soleymani, Method for Electrochemical Detection of Brain Derived Neurotrophic Factor (BDNF) in Plasma, *Anal. Chem.*, 2018, **90**, 8561–8566.

15 A. Gonzalez, M. Gaines, L. Y. Gallegos, R. Guevara and F. A. Gomez, Thread- paper, and fabric enzyme-linked immunosorbent assays (ELISA), *Methods*, 2018, **146**, 58–65.

16 J. D. Bishop, H. V. Hsieh, D. J. Gasperino and B. H. Weigl, Sensitivity enhancement in lateral flow assays: a systems perspective, *Lab Chip*, 2019, **19**, 2486–2499.

17 A. K. Yetisen, M. S. Akram and C. R. Lowe, Paper-based microfluidic point-of-care diagnostic devices, *Lab Chip*, 2013, **13**, 2210–2251.

18 A. L. Tomás, M. P. de Almeida, F. Cardoso, M. Pinto, E. Pereira, R. Franco and O. Matos, Development of a Gold Nanoparticle-Based Lateral-Flow Immunoassay for Pneumocystis Pneumonia Serological Diagnosis at Point-of-Care, *Front. Microbiol.*, 2019, **10**, 267–271.

19 T. Peto and Team, U. C.-L. F. O., COVID-19: Rapid antigen detection for SARS-CoV-2 by lateral flow assay: A national systematic evaluation of sensitivity and specificity for mass-testing, *EClinicalMedicine*, 2021, **36**, 100924.

20 E. M. Hamad, G. Hawamdeh, N. A. Jarrad, O. Yasin, S. I. Al-Gharabli and R. Shadfan, Detection of Human Chorionic Gonadotropin (hCG) Hormone using Digital Lateral Flow Immunoassay, *Annu. Int. Conf. IEEE Eng. Med. Biol. Soc.*, 2018, **2018**, 3845–3848.

21 T. Mahmoudi, M. de la Guardia and B. Baradaran, Lateral flow assays towards point-of-care cancer detection: A review of current progress and future trends, *TrAC, Trends Anal. Chem.*, 2020, **125**, 115842.

22 R. Sambursky, W. F. Davitt, , III, R. Latkany, S. Tauber, C. Starr, M. Friedberg, M. S. Dirks and M. McDonald, Sensitivity and Specificity of a Point-of-Care Matrix Metalloproteinase 9 Immunoassay for Diagnosing Inflammation Related to Dry Eye, *JAMA Ophthalmol.*, 2013, **131**, 24–28.

23 J. Y. Park, B. G. Kim, J. S. Kim and J. H. Hwang, Matrix Metalloproteinase 9 Point-of-Care Immunoassay Result Predicts Response to Topical Cyclosporine Treatment in Dry Eye Disease, *Transl. Vis. Sci. Technol.*, 2018, **7**, 31.

24 J. F. Bergua, L. Hu, C. Fuentes-Chust, R. Alvarez-Diduk, A. H. A. Hassan, C. Parolo and A. Merkoci, Lateral flow device for water fecal pollution assessment: from troubleshooting of its microfluidics using bioluminescence to colorimetric monitoring of generic Escherichia coli, *Lab Chip*, 2021, **21**, 2417–2426.

25 S. Lou, J. Y. Ye, K. Q. Li and A. Wu, A gold nanoparticle-based immunochromatographic assay: the influence of nanoparticulate size, *Analyst*, 2012, **137**, 1174–1181.

26 D. S. Kim, Y. T. Kim, S. B. Hong, J. Kim, N. S. Huh, M.-K. Lee, S. J. Lee, B. I. Kim, I. S. Kim, Y. S. Huh and B. G. Choi, Development of Lateral Flow Assay Based on Size-Controlled Gold Nanoparticles for Detection of Hepatitis B Surface Antigen, *Sensors*, 2016, **16**, 2154.

27 R. C. Murdock, L. Shen, D. K. Griffin, N. Kelley-Loughnane, I. Papautsky and J. A. Hagen, Optimization of a Paper-Based ELISA for a Human Performance Biomarker, *Anal. Chem.*, 2013, **85**, 11634–11642.

28 C.-P. Jia, X.-Q. Zhong, B. Hua, M.-Y. Liu, F.-X. Jing, X.-H. Lou, S.-H. Yao, J.-Q. Xiang, Q.-H. Jin and J.-L. Zhao, Nano-ELISA for highly sensitive protein detection, *Biosens. Bioelectron.*, 2009, **24**, 2836–2841.

29 S. Aydin, A short history, principles, and types of ELISA, and our laboratory experience with peptide/protein analyses using ELISA, *Peptides*, 2015, **72**, 4–15.

30 R. Pan, Y. Jiang, L. Sun, R. Wang, K. Zhuang, Y. Zhao, H. Wang, M. A. Ali, H. Xu and C. Man, Gold nanoparticle-based enhanced lateral flow immunoassay for detection of Cronobacter sakazakii in powdered infant formula, *J. Dairy Sci.*, 2018, **101**, 3835–3843.

31 B. N. Khlebtsov, R. S. Tumskiy, A. M. Burov, T. E. Pylaev and N. G. Khlebtsov, Quantifying the Numbers of Gold Nanoparticles in the Test Zone of Lateral Flow Immunoassay Strips, *ACS Appl. Nano Mater.*, 2019, **2**, 5020–5028.

32 L. Zhang, Y. Mazouzi, M. Salmain, B. Liedberg and S. Boujday, Antibody-Gold Nanoparticle Bioconjugates for Biosensors: Synthesis, Characterization and Selected Applications, *Biosens. Bioelectron.*, 2020, **165**, 112370.

33 A. E. James and J. D. Driskell, Monitoring gold nanoparticle conjugation and analysis of biomolecular binding with nanoparticle tracking analysis (NTA) and dynamic light scattering (DLS), *Analyst*, 2013, **138**, 1212–1218.

34 Y. Gong, J. Hu, J. R. Choi, M. You, Y. Zheng, B. Xu, T. Wen and F. Xu, Improved LFIAs for highly sensitive detection of BNP at point-of-care, *Int. J. Nanomed.*, 2017, **12**, 4455–4466.

35 C. Parolo, A. Sena-Torralba, J. F. Bergua, E. Calucho, C. Fuentes-Chust, L. Hu, L. Rivas, R. Alvarez-Diduk, E. P. Nguyen, S. Cinti, D. Quesada-Gonzalez and A. Merkoci, Tutorial: design and fabrication of nanoparticle-based lateral-flow immunoassays, *Nat. Protoc.*, 2020, **15**, 3788–3816.

36 K. M. Koczula and A. Gallotta, Lateral flow assays, *Essays Biochem.*, 2016, **60**, 111–120.

37 M. Amini, M. R. Pourmand, R. Faridi-Majidi, M. Heiat, M. A. Mohammad Nezhady, M. Safari, F. Noorbakhsh and H. Baharifar, Optimising effective parameters to improve performance quality in lateral flow immunoassay for detection of PBP2a in methicillin-resistant Staphylococcus aureus (MRSA), *J. Exp. Nanosci.*, 2020, **15**, 266–279.

38 A. K. Yetisen, N. Jiang, A. Tamayol, G. U. Ruiz-Esparza, Y. S. Zhang, S. Medina-Pando, A. Gupta, J. S. Wolffsohn, H. Butt, A. Khademhosseini and S. H. Yun, Paper-based microfluidic system for tear electrolyte analysis, *Lab Chip*, 2017, **17**, 1137–1148.

39 C. Ruppert, N. Phogat, S. Laufer, M. Kohl and H.-P. Deigner, A smartphone readout system for gold nanoparticle-based lateral flow assays: application to monitoring of digoxigenin, *Microchim. Acta*, 2019, **186**, 119.

40 G. Beykin and J. L. Goldberg, Molecular Biomarkers for Glaucoma, *Curr. Ophthalmol. Rep.*, 2019, **7**, 171–176.

41 D. Pieragostino, L. Agnifili, V. Fasanella, S. D'Aguanno, R. Mastropasqua, C. Di Ilio, P. Sacchetta, A. Urbani and P. Del Boccio, Shotgun proteomics reveals specific modulated protein patterns in tears of patients with primary open angle glaucoma naïve to therapy, *Mol. BioSyst.*, 2013, **9**, 1108–1116.

42 J. Benitez-Del-Castillo, J. Cantu-Dibildox, S. M. Sanz-Gonzalez, V. Zanon-Moreno and M. D. Pinazo-Duran, Cytokine expression in tears of patients with glaucoma or dry eye disease: A prospective, observational cohort study, *Eur J Ophthalmol*, 2019, **29**, 437–443.

43 A. A. Shpak, A. B. Guekht, T. A. Druzhkova, K. I. Kozlova and N. V. Gulyaeva, Ciliary neurotrophic factor in patients with primary open-angle glaucoma and age-related cataract, *Mol. Vision*, 2017, **23**, 799–809.

44 M. B. Abelson, I. J. Udell and J. H. Weston, Normal human tear pH by direct measurement, *Arch. Ophthalmol.*, 1981, **99**, 301.

45 M. S. Norn, Tear fluid pH in normals, contact lens wearers, and pathological cases, *Arch. Ophthalmol.*, 1988, **66**, 485–489.

46 Y. Azuamah, A. Ugwuoke, G. Ogbonna, N. Ikoro, E. Esenwah and A. Megwas, International Journal of Research Effect of Topical 1% Pilocarpine on the Ocular Tear Film pH, *Int. J. Res.*, 2019, **06**, 120–128.

47 C. Salvisberg, N. Tajouri, A. Hainard, P. R. Burkhard, P. H. Lalive and N. Turck, Exploring the human tear fluid: Discovery of new biomarkers in multiple sclerosis, *Proteomics: Clin. Appl.*, 2014, **8**, 185–194.

48 X. Zhan, J. Li, Y. Guo and O. Golubnitschaja, Mass spectrometry analysis of human tear fluid biomarkers specific for ocular and systemic diseases in the context of 3P medicine, *EPMA J.*, 2021, **12**, 449–475.

49 S. Hagan, E. Martin and A. Enríquez-de-Salamanca, Tear fluid biomarkers in ocular and systemic disease: potential use for predictive, preventive and personalised medicine, *EPMA J.*, 2016, **7**, 15.

50 B. A. Mysona, J. Zhao and K. E. Bollinger, Role of BDNF/TrkB pathway in the visual system: Therapeutic implications for glaucoma, *Expert Rev. Ophthalmol.*, 2017, **12**, 69–81.

51 E. Dekeyster, E. Geeraerts, T. Buyens, C. Van den Haute, V. Baekelandt, L. De Groef, M. Salinas-Navarro and L. Moons, Tackling Glaucoma from within the Brain: An Unfortunate Interplay of BDNF and TrkB, *PLoS One*, 2015, **10**, e0142067.

52 M. Fathy, A. M. Darweesh, S. Sharaf, H. M. El-Hanafi, F. M. Ghaleb, I. A. Fahmy and S. M. Hussein, Brain-derived neurotrophic factor (BDNF) gene polymorphism in a cohort of Egyptian primary open-angle glaucoma (POAG) patients, *Bull. Natl. Res. Cent.*, 2020, **44**, 45.

53 M. E. Pease, S. J. McKinnon, H. A. Quigley, L. A. Kerrigan-Baumrind and D. J. Zack, Obstructed Axonal Transport of BDNF and Its Receptor TrkB in Experimental Glaucoma, *Invest. Ophthalmol. Visual Sci.*, 2000, **41**, 764–774.

54 E. C. Johnson, L. M. H. Deppmeier, S. K. F. Wentzien, I. Hsu and J. C. Morrison, Chronology of Optic Nerve Head and Retinal Responses to Elevated Intraocular Pressure, *Invest. Ophthalmol. Visual Sci.*, 2000, **41**, 431–442.

55 C. Galindo-Romero, F. J. Valiente-Soriano, M. Jiménez-López, D. García-Ayuso, M. P. Villegas-Pérez, M. Vidal-Sanz and M. Agudo-Barriuso, Effect of Brain-Derived Neurotrophic Factor on Mouse Axotomized Retinal Ganglion Cells and Phagocytic Microglia, *Invest. Ophthalmol. Visual Sci.*, 2013, **54**, 974–985.

56 F. Oddone, G. Roberti, A. Micera, A. Busanello, S. Bonini, L. Quaranta, L. Agnifili and G. Manni, Exploring Serum Levels of Brain Derived Neurotrophic Factor and Nerve Growth Factor Across Glaucoma Stages, *PLoS One*, 2017, **12**, e0168565.

57 T. Igarashi, K. Nakamoto, M. Kobayashi, H. Suzuki, Y. Tobita, T. Igarashi, T. Okuda, T. Okada and H. Takahashi, Serum Brain-Derived Neurotrophic Factor in Glaucoma Patients in Japan: An Observational Study, *J. Nippon Med. Sch.*, 2020, **87**, 339–345.

58 A. Ghaffariyeh, N. Honarpisheh, M. H. Heidari, S. Puyan and F. Abasov, Brain-derived neurotrophic factor as a biomarker in primary open-angle glaucoma, *Optom. Vis. Sci.*, 2011, **88**, 80–85.

59 S. Gwyn, A. Mitchell, D. Dean, H. Mkocha, S. Handali and D. L. Martin, Lateral flow-based antibody testing for Chlamydia trachomatis, *J. Immunol. Methods*, 2016, **435**, 27–31.

60 J. B. Roedl, S. Bleich, U. Schlotzer-Schrehardt, N. von Ahsen, J. Kornhuber, G. O. Naumann, F. E. Kruse and A. G. Junemann, Increased homocysteine levels in tear fluid of patients with primary open-angle glaucoma, *Ophthalmic Res.*, 2008, **40**, 249–256.